Temporal Registration of 2D X-ray Mammogram Using Triangular B-splines Finite Element Method (TBFEM)

Kexiang Wang[a], Ying He[a], Hong Qin[a], Paul R. Fisher[b] and Wei Zhao[b]

[a]Center for Visual Computing(CVC)
Department of Computer Science, Stony Brook University
Stony Brook, NY 11794, USA

[b]Department of Radiology
Stony Brook University Hospital
Stony Brook, NY 11794, USA

ABSTRACT

In this paper we develop a novel image processing technique to register two dimensional temporal mammograms for effective diagnosis and therapy. Our registration framework is founded upon triangular B-spline finite element method (TBFEM). In contrast to tensor-product B-splines, which is widely used in medical imaging, triangular B-splines are much more powerful, associated with many desirable advantages for image registration, such as flexible triangular domain, local control, space-varying smoothness, and sharp feature modeling. Empowered by the rigorous theory of triangular B-splines, our method can explicitly model the transformation between temporal mammogram pairs over irregular region of interest(ROI), using a collection of triangular B-splines. In addition, it is also capable of describing C^0 continuous deformation at the interfaces between different elastic tissues, while the overall displacement field is smooth. Our registration process consists of two steps: 1) The template image is first nonlinearly deformed using TBFEM model, subject to pre-segmented feature constraints; 2) The deformed template image is further perturbed by applying pseudo image forces, aiming to reducing intensity-based discrepancies. The proposed registration framework has been tested extensively on practical clinical data, and the experimental results demonstrates that the registration accuracy is improved comparing to using conventional FEMs. Besides, the modeling of local C^0 continuities of the displacement field helps to further increase the registration quality considerably.

Keywords: Image registration, X-ray mammogram, finite-element method(FEM)

1. INTRODUCTION AND BACKGROUND

Breast cancer is one of the most common causes for cancer-related death, with annual mortality of over $400,000$ women worldwide. Taking regular mammographic screening and comparing corresponding mammogram are necessary for early detection of breast cancer, which is also the key to successful treatment. To seek abnormality through comparison, the clinical diagnosis involves either pairs of mammogram from the bilateral breasts of the same patient or a series of mammogram acquired from the same breast at different time. However, the first method tends to be unreliable when the left and right breasts contain significantly different structures. But the latter one, which aims at detection of temporal changes in the same breast, produces more robust results. Unfortunately, a temporal pair of mammogram may vary quite significantly due to the spatial disparities caused by the variety in acquisition environments, including 3D position of the breast, the amount of the pressure applied, etc. Such disparities can be corrected through the process of *Temporal Registration*. This paper contributes to the existing state of the art in temporal registration of digital mammography.

Earliest attempts for mammogram registration typically assumed rigidity and affinity of breast deformation. Yin *et al*[1] align mammograms using an optimal rigid transformation which minimizes the least square error between two group of control points. However, due to the elastic nature of the breast, it's far from correct to

Email: [a]{kwang|yhe|qin}@cs.sunysb.edu, [b]{weizhao|pfisher}@notes.cc.sunysb.edu

match mammograms using solely rigid models. Later, radial basis functions (RBF) based on Thin-plate Spline (TPS)[2] and Cauchy-Navier Spline (CNS)[3] are incorporated to build a global smooth nonrigid transformation from a local displacement vector field representing spatial differences between corresponding control points. However, those registration method depending on control points are prone to failure when the pre-segmentation is accurate enough. To this end, recent techniques tend to incorporate the metrics measuring intensity similarities between corresponding images. Writh *et al*[4] align subregions according to local mutual information, then combine them into a global transformation using TPS. Hadjiiski *et al*[5] propose an automatic regional registration method, which bases on the identification of corresponding lesions in temporal mammogram pairs. A pyramid-based multiresolution technique given by Kostelec *et al*[6] integrates a least square measurement with TPS transformation to match bilateral mammograms. Likewise, Rueckert *et al*[7] hierarchically match corresponding breast images, but using a B-spline based free-form deformation(FFD) technique instead. Due to the large variety of breast tissues and their mechanical behaviors, however, it's more appropriate to register temporal mammograms by utilising model-driven simulation. Pathmanathan *et al*[8] build a patient-specific nonlinear 3D model to predict the tumor location. Kita *et al*[9] simulate the deformation of breasts, and accordingly establish the correspondences between their CC and MLO mammographic views. Richard *et al*[1011] build a 2D FEM model from X-ray mammograms, then conduct the registration by deforming it subject to both feature and intensity-driven constraints.

Our approach is inspired by Richard *et al*'s work.[10] But we employ a novel triangular B-spline finite element method (TBFEM) instead and recover large deformation between temporal mammograms following nonlinear elasticity theory. Triangular B-splines, introduced by Dahmen *et al*,[12] has many favorable features, such as flexible simplex-based domain, space-varying continuities, local control, etc. The most unique one of them is the ability to model local sharp features along in the approximated smooth solution. A example of this is illustrated in Figure.1(c). Therefore, the incorporation of TBFEM within our registration framework gives the following advantages over conventional FEMs: i) The region of interest (ROI) can be accurately described and selected as the registration domain, while the tensor-product B-splines methods[7] necessitate extra efforts to refine the problem domain along the irregular boundaries of ROI. ii) In contrast to other simplex-based elements, such as *Lagrange Polynomials*, our TBFEM offers a global smooth solution (Note that the continuities of the solutions given by traditional Lagrange FEM are not ensured across the element boundaries). iii) Users are allowed to model the spatially varying continuities in the approximated deformation field by manipulating the knot configuration according to pre-identified features. Sharp features may appear in the displacement field when the elastic object contains different materials (see Figure.1(a)(b) for this concept). iv) The accurate simulation of the elastic deformation incorporating material heterogeneity can be achieved by using relatively fewer finite-elements.

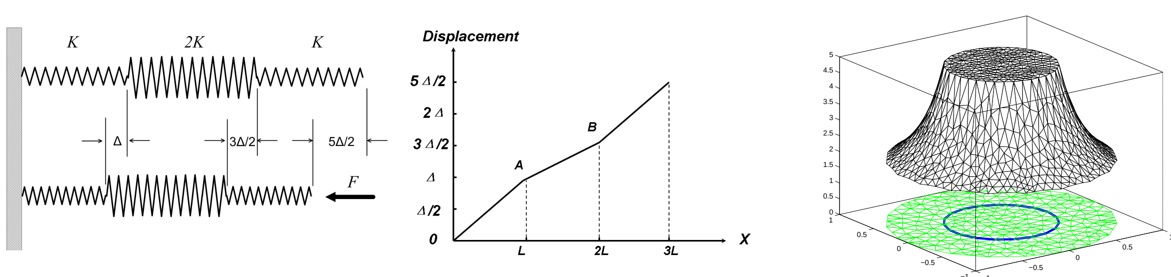

(a) (b) (c)

Figure 1. (a) A one dimensional cascaded spring system system consisting of three springs with stiffness of k, $2k$ and k respectively. When the system is compressed by an external force $\mathbf{F}$, it is deformed and the displacement caused along x-axis is plotted in (b). The sharp features A and B in the displacement profile are built at the joint points between different springs. (c) A functional approximated by a single triangular B-spline, where both C^1 and C^0 continuities co-exist.

2. METHOD

The temporal registration problem can be stated as: given both previous mammogram $\mathcal{T}$ (*template*) and current one $\mathcal{R}$ (*reference*), we are asked to find an optimal transformation ϕ such that the disparities between them are

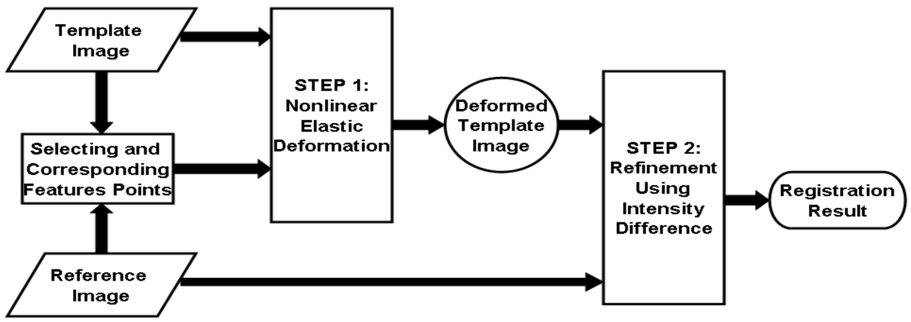

Figure 2. The main flow of the registration process.

reduced maximally. Our registration process(see Figure.2) consists of two consecutive steps, whose details will be developed in the following.

2.1. NONLINEAR ELASTIC DEFORMATION

First, the registration domain Ω is defined over the breast region, which is previously segmented from $\mathcal{R}$ and usually circumvented by the breast skin contour and partial image boundaries. The domain Ω is then triangulated with the user-specified feature lines(see Figure.3(a)). Then we adjust the knots configuration such that the knots collapse to their adjacent sharp features. Thus, C^0 continuity will be successfully modeled in the solution of the recovered displacement field.

The objective of this registration step is to estimate the displacement field $\mathbf{u}^* : \bar{\Omega} \to \mathbb{R}^2$ between $\mathcal{T}$ and $\mathcal{R}$ such that they are aligned as much as possible. Since the breasts compressed during mammography usually undergo large deformation ($> 5\%$), our framework follows nonlinear elastic theory and governs $\mathbf{u}$ by:

$$\begin{cases} \mathbf{A}(\mathbf{u}) = -\nabla \cdot (\mathbf{I} + \nabla \mathbf{u})(\lambda tr(\mathbf{E}(\mathbf{u}))\mathbf{I} + 2\mu \mathbf{E}(\mathbf{u})) = \mathbf{f} \\ \mathbf{u} = \mathbf{u_0} \quad \text{on} \quad \Gamma^d \\ (\mathbf{I} + \nabla \mathbf{u})(\lambda \mathbf{tr}(\mathbf{E}(\mathbf{u}))\mathbf{I} + \mathbf{2}\mu \mathbf{E}(\mathbf{u})) = \mathbf{g_0} \quad \text{on} \quad \Gamma^n \end{cases} \tag{1}$$

in which *St. Venant-Kirchhoff* elastic material is assumed and *Green-St. Venant strain tensor* $\mathbf{E}(\mathbf{u})$ is written in its second order:

$$\mathbf{E}(\mathbf{u}) = \frac{\mathbf{1}}{\mathbf{2}}(\nabla \phi^{\mathbf{T}} \nabla \phi - \mathbf{I}) = \frac{\mathbf{1}}{\mathbf{2}}(\nabla \mathbf{u}^{\mathbf{T}} + \nabla \mathbf{u} + \nabla \mathbf{u}^{\mathbf{T}} \nabla \mathbf{u}) \tag{2}$$

The body force $\mathbf{f}$ does not exist in this step. And λ and μ are *lame* coefficient related to elastic properties.

Due to the nature of registration problems, both *Dirichlet* and *Neumann* conditions in Equation.(1) are dropped, and replaced by a bunches of discretized geometric constraints.[10] Such constraints in our framework consist of two set of control points $\mathcal{P}$ and $\mathcal{Q}$, selected from $\mathcal{R}$ and $\mathcal{T}$ respectively. The majority of the control points come from the breast skin contours and their correspondences are established following the approach proposed by Wirth.[13] Furthermore, salient anatomical structures(vessels branches, nipple, etc.) and pathological points(microcalcification, etc.) are ideal to serve as auxiliary control points. Different from the control points automatically matched on the breast contour using arc-length parametrization, the interior points need to be manually selected and corresponded to each other in our current implementation. Note that such process can be automated by incorporating the technique proposed by Paquerault *et al.*[14] An example of the control points selected from both the template and reference images is shown in Figure.3(b)(c).

The geometric constraints given by $\mathcal{P}$ and $\mathcal{Q}$ are formulated as follows:

$$\phi(\mathbf{p_i}) = \mathbf{q_i} \quad \mathbf{p_i} \in \mathcal{P}, \mathbf{q_i} \in \mathcal{Q}, \mathbf{i} = 1, \ldots, |\mathcal{P}| \tag{3}$$

Where the $\mathbf{p_i}$ and $\mathbf{q_i}$ are corresponding points. These constraints can be viewed as a bunch of displacement vectors from $\mathcal{R}$ to $\mathcal{T}$.

To solve Equation.(1), we linearize it with *Newton's Method*,[15] thus the solution can be approximated incrementally by:

$$\begin{aligned}\mathbf{A}(\mathbf{u^{n+1}}) &\approx \mathbf{A}(\mathbf{u^n}) + \mathbf{A}'(\mathbf{u^n})\delta\mathbf{u^n} = \mathbf{f^n} + \delta\mathbf{f^n} \\ \delta\mathbf{f^n} &= \mathbf{f^{n+1}} - \mathbf{f^n} = \mathbf{A}(\mathbf{u^{n+1}}) - \mathbf{A}(\mathbf{u^n}) \\ \delta\mathbf{u^n} &= \mathbf{u^{n+1}} - \mathbf{u^n}\end{aligned} \tag{4}$$

in which the total displacement field $\mathbf{u}$ is iteratively updated with the increment of $\delta\mathbf{u^n}$, which in turn is the solution of:

$$\mathbf{A}'(\mathbf{u^n})\delta\mathbf{u^n} = \mathbf{f^n} \tag{5}$$

Finally we discretize Equation.(5) in our TBFEM model and solve it in the approximate space $\hat{V} := \text{span}\{B_1, B_2, \ldots, B_N\}$, where B_i denotes the triangular B-spline shape function. After applying *Galerkin Method*,[16] we achieve its discretizaton form written by:

$$\sum_{k=1}^{N} \delta\hat{u}_k^n \int_\Omega \sum_{i,j,p,q=1}^{3} \hat{a}_{ijpq}(\mathbf{u^n})\partial B_k \partial B_l dx = 0 \quad l = 1, \ldots, N \tag{6}$$

in which $\delta\hat{\mathbf{u}}^\mathbf{n} = \sum_{k=1}^{N} \delta\hat{u}_i^n B_i$ and $\hat{a}_{ijpq}$ denotes a FEM discretization operator, the detail of which is available in.[16] The equation above is ill-conditioned unless combined with constraints given in Equation.(3). Suppose that there are total M steps in the elastic deformation, the constraints contributed to the deformation at the n^{th} step are:

$$\sum_{j=1}^{N} B_j(\mathbf{p_i})\delta\hat{u}_j^n = \frac{1}{M-n+1}(\mathbf{q_i} - \mathbf{u^n}(\mathbf{p_i})) \quad i = 1, \ldots, |\mathcal{P}| \tag{7}$$

In essence, the constraints above progressively drag the control points in $\mathcal{R}$ to their corresponding location in $\mathcal{T}$. A linear-interpolation scheme is employed here to predict the position of control points of the next time step. Note that alternative schemes can be incorporated as well.

Substituting Equation.(7) into Equation.(5), we can get a constrained linear problem:

$$\begin{aligned}\mathbf{M^n}\boldsymbol{\Delta}\mathbf{U^n} &= 0 \\ \text{s.t.} \quad \mathbf{C}\boldsymbol{\Delta}\mathbf{U^n} &= \mathbf{D}(\mathbf{U^n}) \\ \mathbf{U^{n+1}} = \mathbf{U^n} + \boldsymbol{\Delta}\mathbf{U^n} \quad &\text{and} \quad \mathbf{U^0} = 0\end{aligned} \tag{8}$$

In current implementation, we first convert the problem above to an unconstrained system by using *Null-space project* technique,[17] then solve it by Conjugate Gradient method(CG). Note that if there is only one time-step assumed for the simulation, the deformation will degenerate to a linear elastic one.

2.2. REFINEMENT WITH INTENSITY DIFFERENCE MINIMIZATION

Let the displacement field obtained in the previous step be $\mathbf{u}^*$, the deformed $\mathcal{T}$ denoted by $\mathcal{T}'(\mathbf{x}) = \mathcal{T}(\mathbf{x} + \mathbf{u}^*)$ which is in rough alignment with $\mathcal{R}$. To further improve the registration results, we perturb $\mathcal{T}'$ with an additional displacement field $\mathbf{v}$ by minimizing a intensity-based metric, which measures the sum of squared difference (SSD) between $\mathcal{T}'$ and $\mathcal{R}$:

$$\mathcal{E}(\mathcal{T}', \mathcal{R}; \mathbf{v}) = \alpha\frac{1}{2}\int_\Omega \|\mathcal{T}'(\mathbf{x} + \mathbf{v}) - \mathcal{R}(\mathbf{x})\|^2 d\mathbf{x} \tag{9}$$

where α weighs the contribution of $\mathcal{E}$.

Similar to Equation.(1), the governing PDE in this step can be written as:

$$\mathbf{A}(\mathbf{v}) = -\nabla \cdot (\lambda tr(\mathbf{E}(\mathbf{v}))\mathbf{I} + 2\mu\mathbf{E}(\mathbf{v})) = \mathbf{f} \tag{10}$$

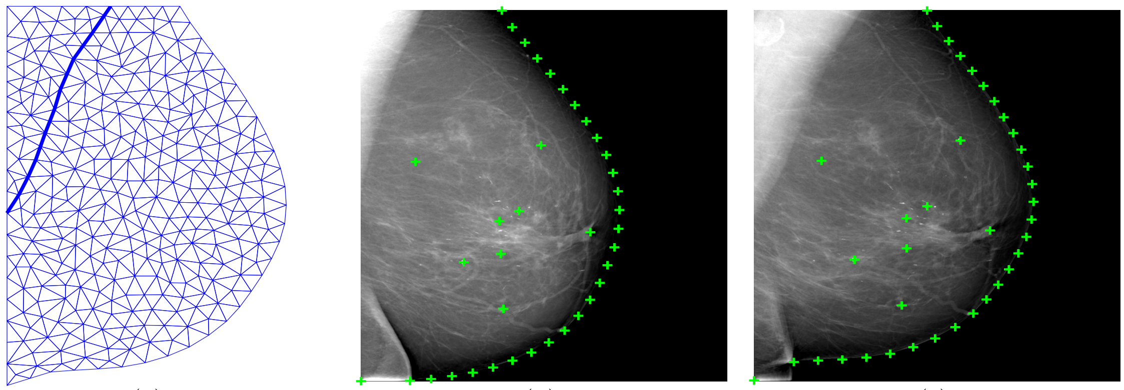

(a) (b) (c)

Figure 3. (a) The triangulated registration domain Ω, where the feature line is highlighted between the pectoral muscles and breast tissue. (b)(c) 8 interior and 29 contour control points in template and reference images respectively.

Note that we assume linear elasticity here because only small deformations are allowed in the second step. Thus, the second order strain tensor is dropped and $\mathbf{A}$ becomes a linear differential operator. Instead of using geometric constraints, we incorporate artificial body forces derived from the minimization of $\mathcal{E}$. In addition, we pin the images at both the upper and lower left corners to avoid unnecessary floating. Consequently, Equation.(10) is discretized to:

$$\mathbf{M^0 V} = \mathbf{F}(\mathbf{V}) \tag{11}$$

where $\mathbf{F}(\mathbf{V})$ denotes the virtual body force, whose elements are:

$$(\mathbf{F}(\mathbf{V}))_i = \alpha \int_{\Omega} (\mathcal{T}(\mathbf{x}+\mathbf{v}) - \mathcal{R}(\mathbf{x}))\nabla\mathcal{T}(\mathbf{x}+\mathbf{v})B_i d\mathbf{x} \tag{12}$$

Note that the stiffness matrix $\mathbf{M^0}$ is identical to that in Equation.(8) at the previous registration step. A gradient descent like algorithm is employed to solve it:

$$\begin{aligned} \mathbf{M^0 \Delta^{n+1}} &= \mathbf{F}(\mathbf{V^n}) && (13)\\ \mathbf{V^{n+1}} &= h\mathbf{\Delta} + (1-h)\mathbf{V} && (14) \end{aligned}$$

associated with a small positive value h. The iteration stops when a predefined threshold ϵ is met:

$$\frac{\mathcal{E}(\mathcal{T},\mathcal{R};\mathbf{V^{n+1}})}{\mathcal{E}(\mathcal{T},\mathcal{R};\mathbf{V^{n}})} < \epsilon$$

3. EXPERIMENT AND RESULTS

Two temporal pairs of 2D X-ray mammograms in MLO views obtained with one year interval (see Figure.4 and Figure.5) are used to test the registration framework proposed in this paper. All of the mammograms have size of 2294×1914, resolution of 94.1μm and 12-bit intensity depth. In the experiment, the images are resized to 1147×957 and their resolution is therefore reduced to 188μm. To suppress the noise as well as speedup the registration process, a gaussian filter with a kernel of 200 pixels is applied to the mammograms before the registration.

The breast region is automatically segmented from each image based on a threshold which is the value of the gray-level corresponding to the first peak in the smoothed histogram of the image. Our registration domain is then defined over the breast region, which is further delaunay-triangulated with pre-identified sharp features as geometric constraints.[18]

For both pair of temporal mammograms, we approximate the underlying displacement field using second order triangular B-splines, in which sharp features are naturally accommodated. A simple heterogeneous model

Case Study (Image registration)		TBFEM with sharp feature modeling	TBFEM without sharp feature modeling	2nd-order Lagrange triangular FEM
Case-1	1st-step registration	86.41%	86.29%	85.93%
	2nd-step registration	86.45%	86.32%	85.97%
Case-2	1st-step registration	94.69%	94.66%	94.56%
	2nd-step registration	94.72%	94.69%	94.58%

Table 1. The registration quality is measured by the post-registration improvement between template image $\mathcal{T}$ and reference image $\mathcal{R}$, which is formulated as $(|\mathcal{T}-\mathcal{R}|^2-|\mathcal{T}_*-\mathcal{R}|^2)/|\mathcal{T}-\mathcal{R}|^2$ where $\mathcal{T}_*$ denotes the new $\mathcal{T}$ after the registration is conducted. In Case-1, there are 2514 DOFs with 600 triangular elements, and for Case-2, there are 2600 DOFs with 619 triangles.

is incorporated with TBFEM to model different elastic material in mammograms. The Young's Modules of $E = 10^4$ and $E = 10^2$ are assigned to pectoral muscles and breast region respectively to model stiff and soft tissue. These values are chosen empirically and only their ratio matters in the first registration step, in which there are no Neumann conditions involved.[19] Since it is learnt from previous researches that the breasts are highly compressible, we choose poisson rate ν as 10^{-10}.

During first registration step, control points are selected automatically on the parameterized breast skin contours and manually from the breast interior region. 29 pairs of contour points and 8 pairs of interior points are picked for the first experimental case, while 33 and 6 pairs respectively for the second. The total nonlinear deformation is divided into 20 time steps; In the second step, the regularization term, weighted by the Young's Module E, counteracts the artificial image forces, whose magnitude is controlled by the coefficient α. Choosing correct values for these registration parameters is essential to the success of our algorithm. In our case studies, we empirically set α to 10^{-3} and h to 10^{-2}, and receive satisfactory results as well as adequate numerical stabilities. The registration result of both experiments are illustrated in Figure.4. and Figure.5.

To evaluate our approach, we quantitatively compare it with two other similar registration methods. One of them is also based on TBFEM but without sharp features modeling (*i.e.*knots are all fixed), the other uses second order *Lagrange* triangular elements instead. The experimental results are documented in Table.1 where the registration qualities are measured by the post-registration improvement between template and reference images. It is noticeable that the pre-registration disparity is mainly reduced in the deformation step while the second registration step makes only small contribution to the final result. The reason is that the salient information provided by X-ray mammograms are apt to trap the intensity-based optimization within local minima. We also find that the registration quality in our framework can be improved by incorporation of prior knowledge of feature lines. However, these improvements seem small in Table.1 because of the massive pre-registration error between template and reference images. Compared with conventional triangular FEM (Lagrange triangular FEM) with the same degree of freedom (DOF) and degree of order, TBFEM can delineate the recovered deformation field more accurately, and thus is superior in our simulation-based registration framework.

Our algorithm was implemented with MSVC++. The experiment was performed on a platform with 2.8GHz CPU and 1G RAM. Each step of nonlinear elastic deformation takes up to 10 seconds. While during the refinement stage, each iteration costs about 3 minutes which stops after 20 steps or so.

4. CONCLUSION AND FUTURE WORK

In this paper, we presented a simulation-based registration framework for temporal pair of 2D x-ray mammograms. A novel triangular B-spline finite element method(TBFEM) is incorporated to accurately model the recovered deformation, as well as the sharp features between different tissue properties using the technique of knots collapsing. Our registration algorithm employs a two-stepped scheme: the massive disparities between temporal mammograms are first reduced through a nonlinear elastic simulation; then the mapping between template and reference images is further refined according to intensity-based information. The results of our experiment have also shown that the TBFEM incorporated with our framework is superior to traditional FEM method by improving registration quality considerably.

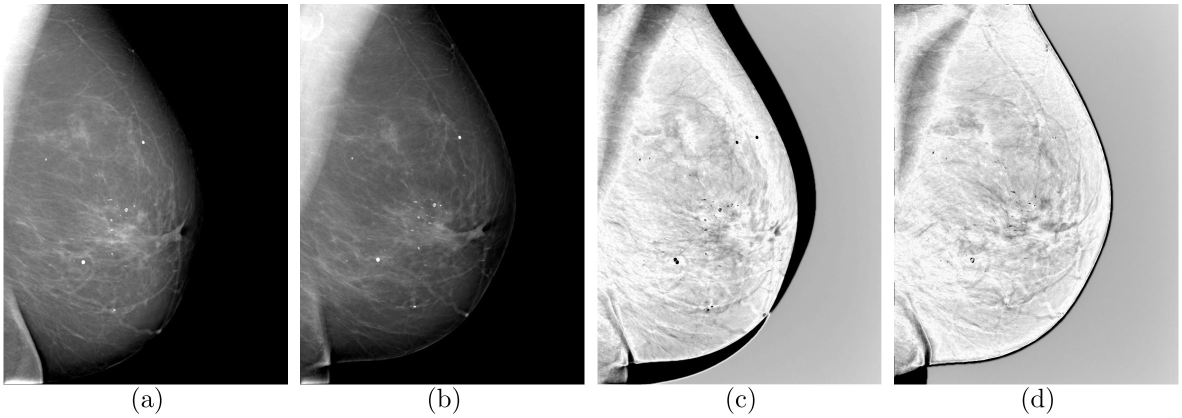

Figure 4. Image registration of Case-1 study (a) Template Image $\mathcal{T}$ (b) Reference Image $\mathcal{R}$ (c) Pre-registered error (d) Post-registered error after two-step registration technique is applied

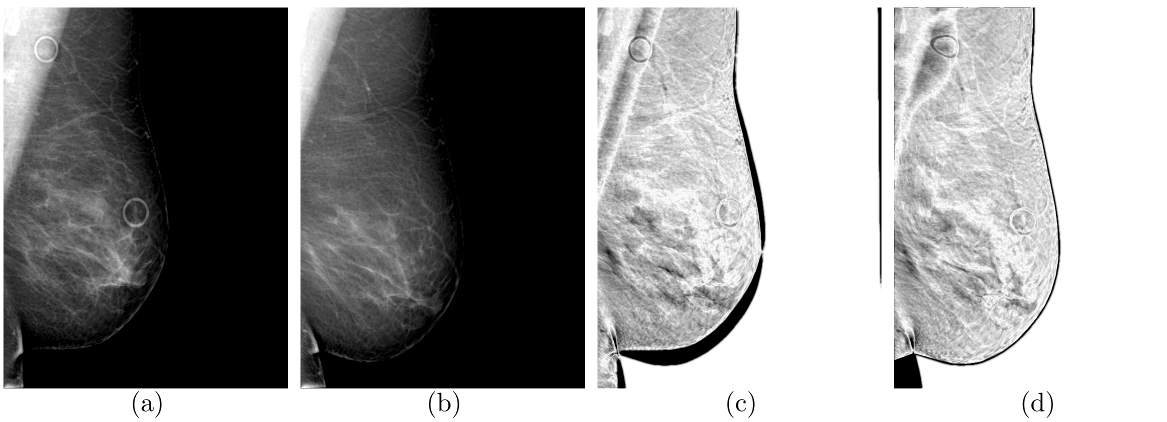

Figure 5. Image registration of Case-2 study (a) Template Image $\mathcal{T}$ (b) Reference Image $\mathcal{R}$ (c) Pre-registered error (d) Post-registered error after two-step registration technique is applied

Our current simulation-based registration method only considers tow dimensional mammograms, which may fail if a lot of out-of-plane motion generated are produced the mammography. To extend current TBFEM into three dimension can simulate the behavior of the breast more accurately, which is the focus of our future work. Advanced measurement of intensity similarities or dissimilarities(*e.g.*mutual information and normalized correlation), need to be incorporated for better tumor detection. Although we only coupled a simple heterogenous elastic model with current TBFEM, triangular B-splines is capable of modeling much more sophisticated material distribution.[20] Nevertheless, the work presented in this paper gives the first successful application of TBFEM in medical imaging. Due to its unique and favorable features, such as flexible triangular domain, space-varying smoothness, etc, TBFEM is a promising tool for modeling of imaging data, simulation of human bodies and many other clinical tasks in the future.

ACKNOWLEDGMENTS

We gratefully acknowledge financial support from the NIH (1 R01 EB002655-01) and the U.S. Army Breast Cancer Research Program (W81XWH-04-1-0554).

REFERENCES

1. F.-F. Yin, M. L. Giger, K. Doi, C. J. Vyborny, and R. R. Schmidt, "Computerized detection of masses in digital mammograms," *Med. Phy.* **32**(3), pp. 445–452, 1994.

2. M. Sallam, *Image unwarping and difference analysis: a technique for detecting abnormalities in mammograms.* PhD thesis, University of South Florida, USA, 1997.
3. M. Writh and C. Choi, “Mammogram registration using the cauchy-navier spline,” in *SPIE Medical Imaging*, **4322**, pp. 1654–1665, 2001.
4. M. Writh, J. Narhan, and D. Gray, “Nonrigid mammogram registrationg using mutual information,” in *SPIE Medical Imaging*, **4684**, pp. 562–573, 2002.
5. L. Hadjiiski, H. Chan, B. Sahiner, N. Petrick, and M. A. Helvie, “Automated registration of breast lesions in temporal pairs of mammograms for interval changes analysis–local affine transformation for improved localization,” *Med. Phys.* **28**(6), pp. 1070–1079, 2001.
6. P. J. Kostelec, J. B. Weaver, and D. M. Healy, “Multiresolution elastic image registration,” *Med. Phys.* **25**(9), pp. 1593–1604, 1998.
7. D. Rueckert, L. I. Sonoda, C. Hayes, D. L. G. Hill, M. O. Leach, and D. J. Hawkes, “Nonrigid registration using free-form deformation: application to breast mr images,” *IEEE Trans. on Med. Imaging* **18**(8), pp. 712–721, 1999.
8. P. Pathmanathan, D. Gavaghan, J. Whiteley, S. M. Brady, M. Nash, P. Nielsen, and V. Rajagopal, “Predicting tumore location by simulating large deformation of the breast using a 3d finite element model and nonlinear elasticity,” pp. 217–224, 2004.
9. Y. Kita, R. Highnam, and M. Brady, “Correspondence between different view breast x-rays using a simulation of breast deformation,” in *CVPR*, pp. 700–707, June 1998.
10. F. Richard and C. Graffigne, “An image-matching model for the registration of temporal or bilateral mammogram pairs,” pp. 756–762, June 2000.
11. F. Richard and L. Cohen, *A new Image registration technique with free boundary constraints : application to mammography*, vol. 89, 2003.
12. W. Dahmen, C. A. Micchelli, and H. P. Seidel, “Blossoming begets *b*-spline bases built better by b-patches,” *Mathematics of Computation* **59**(199), pp. 97–115, 1992.
13. M. Wirth, *A nonrigid approach to medical image registration: matching images of the breast.* PhD thesis, RMIT University, Victora, Australia, June 1999.
14. S. Paquerault, L. M. Yarusso, J. Papaioannou, Y. Jiang, and R. M. Nishikawa, “Radial gradient-based segmentation of mammographic microcalcifications,” *Med. Phys.* **31**(9), pp. 2648–2657, 2004.
15. C. T. Kelley, *Iterative methods for linear and nonlinear equations*, SIAM, Philadelphia, 1995.
16. P. G. Ciarlet, *Mathematical elasticity, Volume 1: Three-dimensional elasticity, Volume 20 of studies in mathematics and its applications*, North-Holland, Amsterdam, 1988.
17. P. Gill, W. Murray, and M. Wright, *Practical optimization*, Academic Press, 1981.
18. J. R. Shewchuk, “Triangle: engineering a 2d quality mesh generator and delaunay triangulator,” in *Proc. of 1st Worksh. Applied Computational Geometry*, pp. 124–132, May 1996.
19. M. M. Doyley, P. M. Meaney, and J. C. Bamber, “Evaluation of an iterative reconstrution method for quantitative elastography,” *Phys. Med. Biol.* **45**, pp. 1521–1540, 2000.
20. J. Hua, Y. He, and H. Qin, “Multiresolution heterogeneous solid modeling and visualization using trivariate simplex splines,” in *9th ACM Symposium on Solid Modeling and Application*, pp. 47–58, June 2004.